J Mater Sci: Mater Med (2013) 24:1843–1851
DOI 10.1007/s10856-013-4954-x

Synthesis and characterization of chitosan–multiwalled carbon nanotubes/hydroxyapatite nanocomposites for bone tissue engineering

Li Chen · Jingxiao Hu · Xinyu Shen · Hua Tong

Received: 26 September 2012 / Accepted: 6 May 2013 / Published online: 28 May 2013

Abstract Chitosan–multiwalled carbon nanotubes/hydroxyapatite nanocomposites were synthesized by a novel in situ precipitation method. The electrostatic adsorption between multiwalled carbon nanotubes and chitosan was investigated and explained by Fourier transform infrared spectroscopy analysis. Morphology studies showed that uniform distribution of hydroxyapatite particles and multiwalled carbon nanotubes in the polymer matrix was observed. In chitosan–multiwalled carbon nanotubes/hydroxyapatite nanocomposites, the diameters of multiwalled carbon nanotubes were about 10 nm. The mechanical properties of the composites were evaluated by measuring their compressive strength and elastic modulus. The elastic modulus and compressive strength increased sharply from 509.9 to 1089.1 MPa and from 33.2 to 105.5 MPa with an increase of multiwalled carbon/chitosan weight ratios from 0 to 5 %, respectively. Finally, the cell biocompatibility of the composites was tested in vitro, which showed that they have good biocompatibility. These results suggest that the chitosan–multiwalled carbon nanotubes/hydroxyapatite nanocomposites are promising biomaterials for bone tissue engineering.

1 Introduction

Bone repair or regeneration is a pervasive and challenging clinical problem in orthopaedic surgery. Nowadays, more and more people are being afflicted with bone defects. Autogenic and allogenic bones are commonly used to deal with bone defects. However, it's well known that autogenic bones needs secondary surgery to procure donor bone from the patient's own body and allogenic bone bears risk of infections and immune responses [1]. Thus, patient's needs have spurred the development of artificial bone tissue material preparation, transplantation, surgical reconstruction and the use of artificial prostheses [2–7].

Chitosan (CS) is a randomly partially deacetylated form of chitin, the β-(1,4)-linked polymer of *N*-acetyl-D-glucos-2-amine, extracted from crustacean exoskeletons. Chitosan is biocompatible and can be degraded by enzymes in human body, and the degradation product is nontoxic [8]. It has been widely used in many biomedical researches, such as bone tissue engineering [9–12], nerve [13–15], retinal tissue engineering [16], drug carriers [17] and blood vessel [18]. However, because the bioactivity of chitosan isn't good enough for bone tissue engineering, it is often combined with other bioactive materials. Hydroxyapatite (HA), a main inorganic component of bone, is a biologically active calcium phosphate ceramic that is used in surgery to replace and mimic bone. While HA's bioactivity means it has a significant ability to promote bone growth along its surface, its mechanical properties are insufficient for major load-bearing devices [19]. To solve this problem, reinforcing phases are usually introduced into composites, including ZrO_2 [20], polyamide 66 [21], silk fibroin [22] and polylactic acid [23].

An ideal reinforcement material would impart mechanical integrity to the composite at low loadings, without diminishing its bioactivity [19]. Due to their small dimensions, high aspect ratio (length to diameter), and high strength and stiffness, multiwalled carbon nanotubes (MWNTs) have aroused some researchers' interest in the biomedical area [24–29].

L. Chen · J. Hu · X. Shen (✉) · H. Tong (✉)
Key Laboratory of Analytical Chemistry for Biology and Medicine, Ministry of Education, College of Chemistry and Molecular Sciences, Wuhan University, Wuhan 430072, People's Republic of China
e-mail: shenxy@whu.edu.cn

H. Tong
e-mail: tonghua@whu.edu.cn

Especially, MWNTs and HA are often applied in composite materials to improve their mechanical properties and bioactivity. Herein, chitosan–multiwalled carbon nanotubes/hydroxyapatite (CS-MWNTs/HA) nanocomposite was synthesized by a novel in situ precipitation method to get further applications for bone tissue engineering.

In the parent work, we firstly dispersed MWNTs in chitosan via ultrasonic method. Later, in situ precipitation approach was employed to deposit HA in the hydrogel of chitosan–multiwalled carbon nanotubes (CS-MWNTs) [23]. To the best of our knowledge, there are little reports on preparing CS-MWNTs/HA nanocomposites through in situ precipitation technology which endowed synthesized composites with unique morphology ultrafine nano-HA particles dispersed in organic template homogenously. Meanwhile, it's worth of noting that this method had another important merit that the products had no other impure inorganic component except HA in composites [30, 31]. This work aims to put forward a new method to prepare CS-MWNTs/HA nanocomposites which combines good biocompatibility with high strength.

2 Materials and methods

Chitosan (Mw 1,000,000) was obtained from Golden-Shell Biochemical Co. (Zhejiang, China) with 95 % degree of the deacetylation. Carboxylic multiwalled carbon nanotube (outer diameter 10–20 nm, length 5–15 μm) was purchased from Shenzhen Nanotech (Shenzhen, China). Calcium nitrate tetrahydrate ($Ca(NO_3)_2{\cdot}4H_2O$), diammonium hydrogen phosphate ($(NH_4)_2HPO_4$), glutaraldehyde, acetic acid and ammonia were purchased from Sinopharm Chemical Reagent Co., Ltd. (Shanghai, China) and were all of analytical grade. All chemicals were used as received without any further purification. Deionized ultrapure water was used throughout the experiment.

2.1 Synthesis of CS-MWNTs/HA nanocomposites by in situ precipitation

Composites of CS-MWNTs/HA were synthesized by the following procedures. CS solution was prepared by dissolving 0.24 g CS in 40 ml of acetic acid solution (2 vol%) with stirring at 45 °C until it became perfectly transparent. Simultaneously, MWNTs were dispersed in ethanol and sonicated for 10 min. Subsequently, CS solution was added into the MWNTs dispersion and sonicated for 1.5 h. Then 1.32 g $Ca(NO_3)_2{\cdot}4H_2O$ and 0.44 g $(NH_4)_2HPO_4$ were added to the CS-MWNTs mixture under agitation until the salts were entirely dissolved. Next, 0.2 ml glutaraldehyde (25 wt%) was added to the previous mixed solution as a crosslinker and the solution was stirred at 80 °C until an black hydrogel was produced. The as-synthesized hydrogel was stored under ambient conditions for 24 h to achieve complete crosslinking. It was then kept in ammonia solution for 24 h at 25 °C. Under this alkaline condition, HA precipitated within the hydrogel matrix gradually [30, 31]. The in situ precipitation route can be represented by the following chemical reaction:

$$10Ca^{2+} + 6HPO_4^{2-} + 8OH^- + Ca_{10}(PO_4)_6(OH)_2(\downarrow) + 6H_2O \ (pH > 10)$$

After soaking in ammonia, the composite was rinsed with distilled water until the pH of the eluate was about 7. By changing the weight ratios of MWNTs/CS to 2, 3, 4 and 5 %, a series of CS-MWNTs/HA nanocomposites were prepared.

2.2 Synthesis of CS/HA nanocomposites by in situ precipitation

CS/HA nanocomposites as control samples were also prepared by in situ precipitation. The procedures are the same as described in Sect. 2.1, but without the addition of MWNTs. An opaque composite of CS/HA was produced.

2.3 Characterization

The products were characterized with environmental scanning electron microscopy (SEM, Quanta200, FEI, Holland), wide angle X-ray diffraction analysis (XRD, X'pert PRO, Panalytical, Holland), field emission transmission electron microscope (2010FEF, JOEL, Japan) and Fourier Transform Infrared Spectrometer (FT-IR, Nicolet5700, America).

Mechanical properties tests were measured at room temperature by a universal testing machine (SHIMADZU, AGS-J, Japan) at a crosshead speed of 0.5 mm/min. Elastic modulus was calculated as the slope of the initial linear portion of the stress–strain curve.

Samples of CS/HA and CS-MWNTs/HA nanocomposites were made into circular discs suitably sized (diameter 5 mm, height 2 mm). The MC3T3-E1 cells (2.0×10^4 cells/well) were seeded on each discs placed in the 96-well plates (Corning Life Sciences). Cells cultivated in the same wells without samples were used as a control. Plates were incubated in Dulbecco's modified Eagle medium (DMEM) containing 10 % fetal bovine serum (FBS) at 37 °C in a 5 % CO_2 incubator for 7 days, and the cell viability was studied using cell counting kit-8 assay (CCK-8; Dojindo Laboratories, Japan) according to the manufacturer's instructions. After 3 and 7 days of culture, nanocomposites were gently washed with PBS and then 2 mL of DMEM containing 10 % CCK-8 was added per well. The disks were incubated at 37 °C for 3 h. After incubation, the

supernatant was transferred to a 96-well plate and the optical density (OD) was measured at 450 nm using an ELX808 Ultra Microplate Reader (Bio-Tek Instruments, Inc., America).

Behaviors of MC3T3-E1 cells on various CS-MWNTs/HA nanocomposites were studied by SEM. After cultivation for 2 days, composites grown with cells were washed twice with PBS, and cells were fixed with 2.5 % glutaraldehyde under 4 °C overnight. Fixed samples were dehydrated by ethanol in an increasing concentration gradient (30, 50, 70, 90, 95 and 100 vol%), followed by lyophilization. The dried samples were glued onto copper stubs, and sputter coated with gold prior to SEM observation.

3 Results

3.1 Compositional properties and morphology of CS-MWNTs/HA nanocomposites

As shown in Fig. 1a, the spectrum for the MWNTs showed absorbances at 1,740 and 1,120 cm^{-1}, which were ascribed, respectively, to the C=O and C–O stretching of carboxylic acids. The peaks at 672 and 3,729 cm^{-1} are corresponding to the bending vibration and stretching vibration of –OH, respectively. For the CS/HA composite (Fig. 1c) and the CS-MWNTs/HA composite (Fig. 1b), the bands at 1,092, 1,035, 961, 603 and 566 cm^{-1} corresponded to different vibration modes of phosphate group in HA, while the bands at 3,570 and 632 cm^{-1} represented hydroxyl group as stretching and bending vibration. Bands assigned to carbonate group at 1,482, 1,452, 1,424 and 874 cm^{-1} were also observed. This agreed with the fact that HA crystals prepared using the precipitation method contained carbonate ions [32]. From the FTIR spectra of the CS/HA composite (Fig. 1c), the bands around 1,638 and 1,566 cm^{-1} were assigned to amide I (C=O), amino ($–NH_2$) of CS, respectively. In the case of CS-MWNTs/HA composite, the main characteristic peaks of MWNTs and CS coexist and no new peaks appear, reflected by the presence of the peak at 1,740 cm^{-1} associated with MWNTs and the peaks at 1,638 cm^{-1} related to CS (Fig. 1b). This confirms that electrostatic adsorption may occur between the protonated amine groups of CS and the carboxylate groups on the MWNTs, which helps MWNTs to disperse in the CS uniformly.

Figure 1d exhibits the XRD results of the CS-MWNTs/HA composite. The peak positions are matching closely the diffraction peaks of stoichiometric HA (verified by PDF Card No. 9-432). It is evident that three intense peaks of crystal phases at 25.9°, 32° and 39.7° (2θ), which are assigned to (002), (211) and (310) of crystalline HA, respectively. The XRD pattern of the CS-MWNTs/HA nanocomposite showed broad peaks with poor crystallinity around the characteristic diffraction region near to 32° (2θ), which suggested low crystallinity of HA in the CS-MWNTs/HA nanocomposite. This crystallographic structure of the CS-MWNTs/HA nanocomposite was more similar to natural bone mineral (biological apatite) [33]. Therefore, the HA nanocrystallites in the CS-MWNTs/HA nanocomposite have more similarities with natural bone mineral in terms of the degree of crystallinity. However, no MWNTs peaks were found in the XRD patterns, which may result from that the characteristic peak of MWNTs and the diffraction peak of HA is coincident and the intensity of HA diffraction peak is so strong.

As shown in Fig. 2, it can be seen that the MWNTs absolutely precipitate after nine days standing. After MWNTs sonication in the CS solution in contrast, it can be well dispersed in the CS solution for nine days, which may result from that electrostatic adsorption between MWNTs and CS hinders MWNTs agglomeration.

SEM micrograph observations of CS-MWNTs/HA composite (Fig. 3c) showed that the interface between the inorganic and organic phases was indistinguishable, because the inorganic crystals have a high affinity with the

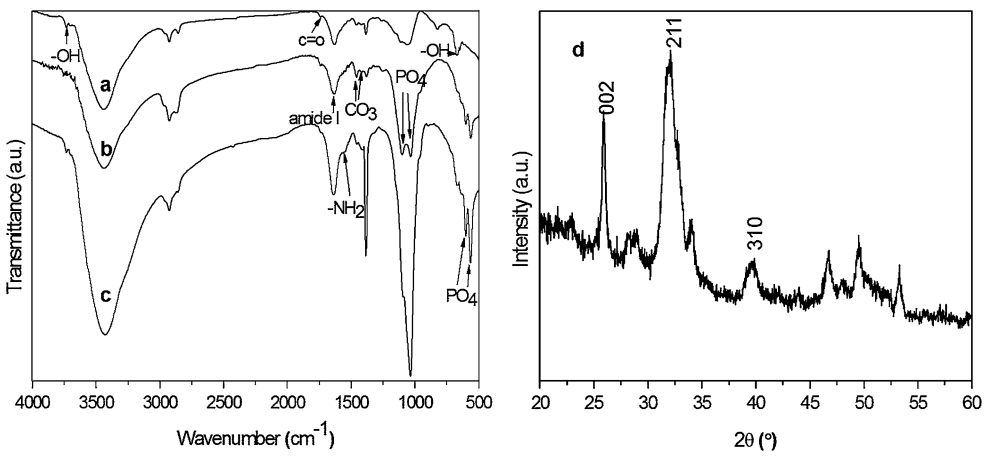

Fig. 1 FTIR spectra of *a* MWNTs, *b* the CS-MWNTs/HA composite, *c* the CS/HA composite, and **d** XRD pattern of the CS-MWNTs/HA composite

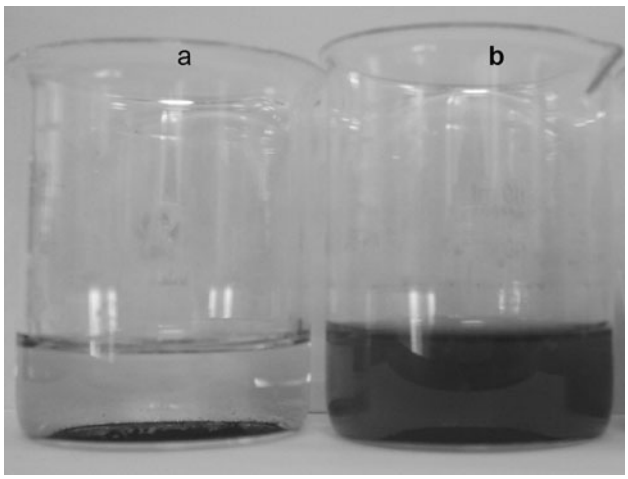

Fig. 2 The appearance of samples in 2 % (V/V) HAc after nine days; **a** MWNTs, **b** CS-MWNTs

CS-MWNTs matrix. No delamination was observed between the inorganic phase and the organic phase. This intimate bonding between inorganic particles and organic matrix may help to improve the mechanical properties of the composite. It is difficult to get this kind of decentralization effect by normal mechanical mixing methods. Meanwhile, the dispersion of MWNTs was more harmonized in matrix, which is also beneficial for the composites to enhance its mechanical properties.

SEM image of MWNTs (Fig. 3a) presented that the diameters of MWNTs were about 10 nm. From the SEM results of the CS/HA composite (Fig. 3b), it could be observed that only spheroidal HA nanoparticles dispersed in the CS matrix. However, Fig. 3c showed that the inorganic particles exhibited as nanosized rods. Figure 3e definitely illuminated the formation mechanism of CS-MWNTs/HA nanocomposites. In this work, chitosan hydrogel played an important role in the superfine interaction of inorganic and organic phases through the compartment effect of its interior. These compartments also limited the migration of the MWNTs and caused them to disperse homogeneously throughout the CS hydrogel. With the increase of pH after the addition of ammonia, carboxyl groups of MWNTs may partly begin to act as nucleation center for HA formation. These negatively charged carboxyls can contact with Ca^{2+} to form the electrovalent bonds. The PO_4^{3-} can bond Ca^{2+} through strong electrostatic interaction and thus comes into being a large scale of local supersaturation microenvironment. Lastly, the HA crystals initiate their further growth and precipitate in the network of hydrogel template to form a direct sequenced minerals.

On the other hand, the CS hydrogel template alone was unable to mediate nanosized rods in the CS/HA composite. Because there is no MWNTs template, Ca^{2+} and PO_4^{3-} ions tended to interact with carbonyl and amino groups on the compartment walls of the CS hydrogel network. These heterogeneous nucleation sites were irregular, it was hard to form a high electrostatic field concentration. In addition, TEM was used to confirm the presence of MWNTs in the CS-MWNTs/HA composite. In Fig. 3d, it's evident that MWNTs existed in the CS-MWNTs/HA composite indeed and the diameters of MWNTs were about 10 nm. This result corresponds to SEM image of MWNTs (Fig. 3a).

3.2 Mechanical properties of CS-MWNTs/HA nanocomposites

The mechanical properties of the CS/HA and CS-MWNTs/HA composite with different MWNTs/CS weight ratios were tested by a universal testing machine. Figure 4a–e shows the stress–strain data of samples with different MWNTs/CS weight ratios ranging from 0 to 5 %. All the tests were conducted under a compressive load at 0.5 mm/min. The data demonstrated that all the samples presented similar stress–strain behavior. The stress increased sharply during the initial stage of compression and then reduced subsequently until finally fracture was reached. Compared with the CS/HA composites, the CS-MWNTs/HA composites obviously exhibited higher stress at same strain. Clearly, the loading level of MWNTs has a profound effect on the mechanical properties. It is strongly obvious that the elastic modulus and compressive strength increased sharply from 509.9 to 1089.1 MPa and from 33.2 to 105.5 MPa with an increase of MWNTs/CS weight ratios from 0 to 5 %, respectively (Fig 4f, g). Some of the factors leading to the enhancement in mechanical properties of CS-MWNTs/HA composites could be ascertained: (1) the strong interfacial interaction between inorganic and organic phase gained from employment of the in situ precipitation method; (2) the introduction of MWNTs, which has a high mechanical property, as a reinforcement phase; (3) uniform dispersion of MWNTs in the polymer matrix. However, it has been reported that natural bone has a much higher modulus (20 GPa) [34] than that of CS-MWNTs/HA composites. Therefore, if the interfacial bonding between MWNTs and CS can be enhanced, the CS-MWNTs/HA composites may show highly modulus. Then the CS-MWNTs/HA composites may even match the properties of natural bones and widely used in the surgical applications.

3.3 Cell morphology and proliferation on CS-MWNTs/HA nanocomposites

Morphologic changes of cells that were contacted biomaterials or biomaterial extracts indicate their toxicity [35]. In

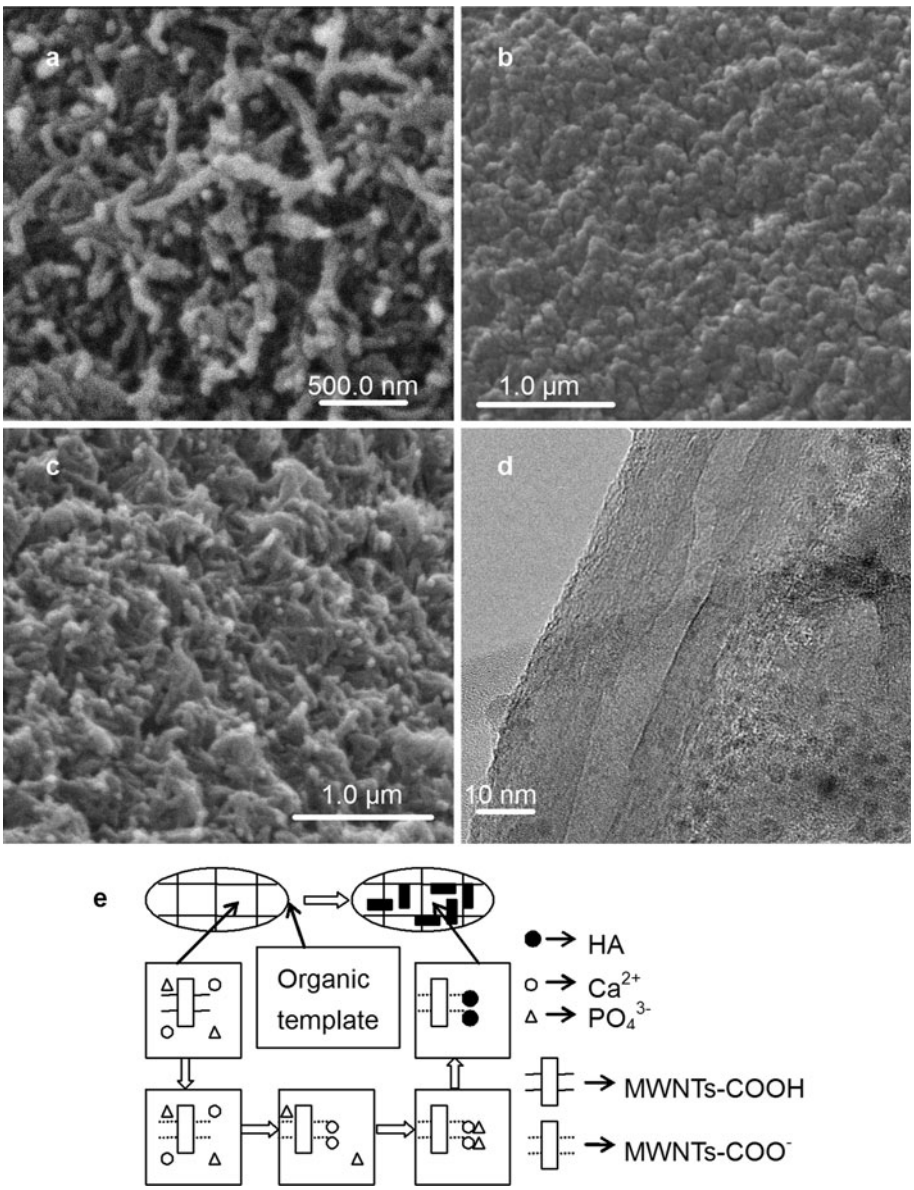

Fig. 3 SEM micrograghs of **a** MWNTs, **b** the CS/HA composite, **c** the CS-MWNTs/HA composite, **d** TEM micrographs of the CS-MWNTs/HA composites, and **e** scheme of the formation mechanism of CS-MWNTs/HA nanocomposites

this work, cells morphologic analysis was applied to evaluate the cytotoxicity of the CS-MWNTs/HA composites. Figure 5a–e show representative SEM morphologies of preosteoblast MC3T3-E1 cells grown on the CS-HA composites and CS-MWNTs/HA composites with different MWNTs/CS weight ratios after 2 days. No matter on the CS-HA composites or on the CS-MWNTs/HA composites with different MWNTs/CS weight ratios, the cells were spread out and had some filopods. Meanwhile, the cells presented fusiform and polygonal morphology. These results demonstrate that preosteoblast MC3T3-E1 cells attachment and adhesion on the surface of the CS-MWNTs/HA composites is good and the CS-MWNTs/HA composites possess non-cytotoxicity.

Cell proliferation on CS-MWNTs/HA nanocomposites was quantified by using CCK-8 assay. Figure 5f presents the proliferation of preosteoblast MC3T3-E1 cells on CS/HA and CS-MWNTs/HA composites with different MWNTs/CS weight ratios after 3 and 7 days of culture. It is worth of noting that MC3T3-E1 cell proliferation on CS-HA or CS-MWNTs/HA surface at 7 days of culture is higher than that at 3 days of culture, indicating good in vitro biocompatibility of CS-HA and CS-MWNTs/HA nanocomposites. Besides, when compared with CS-HA surface, significantly enhanced osteoblast proliferation was observed on CS-MWNTs/HA surface.

4 Discussion

Traditional therapeutic approaches in treating large bone defects include bone grafts [36] and transplants [37]

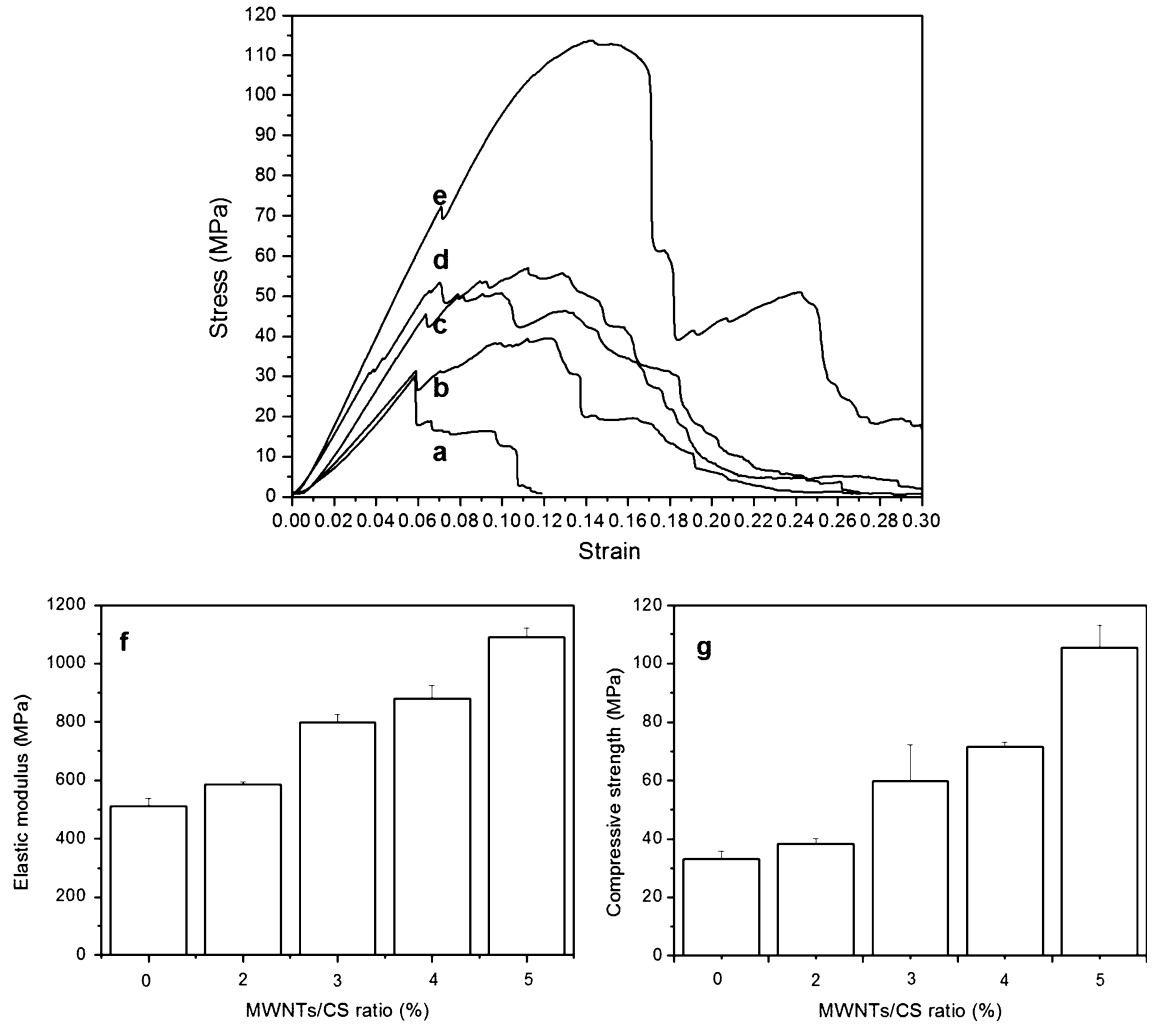

Fig. 4 Compressive stress–strain curves of CS-MWNTs/HA composites with different MWNTs/CS weight ratios: *a* blank, *b* MWNTs/CS = 2 %, *c* MWNTs/CS = 3 %, *d* MWNTs/CS = 4 %, *e* MWNTs/CS = 5 %, and mechanical properties curves of CS-MWNTs/HA composite with different MWNTs/CS weight ratios: **f** elastic modulus-MWNTs/CS weight ratio *bar graph*; **g** compressive strength-MWNTs/CS weight ratio bar graph (n = 3)

(autologous—from the iliac bone or fibular grafts, allograft—fresh or frozen after cleaning, or xeno-grafts). Autografts have achieved various degrees of success in treating bone defects. However, the autograft is limited by the donor site morbidity, prolonged rehabilitation, increased risk of deep infection and restricted availability. Allografts might cause potential risks of transmitted diseases such as HIV or contamination [38, 39]. Thus, more and more researchers have studied on organic/inorganic composite biomaterials alloplastic grafts in recent years. In this study, we established the novel and simple in situ precipitation method of preparing CS-MWNTs/HA composites.

It has been reported that CS/HA composites show good biocompatibility and favorable degradation [40, 41]. Furthermore, it has been demonstrated that CS/HA composites can enhance tissue regenerative efficacy and osteoconductivity [42, 43]. The techniques nowadays used to synthesize CS/HA composites are mostly mechanical mixing [44], co-precipitation [45] and an alternate soaking process [46]. However, there is a common disadvantage of all these approaches that inorganic particles cannot be distributed within the organic matrices at the nanolevel, and this has led to poor mechanical properties and limited their applications. In our previous study [23, 30, 31], we demonstrated the novel and simple in situ precipitation method to promote high-affinity nucleation and growth of hydroxyapatite in polymer hydrogel. Compared with other methods, the advantage of in situ precipitation is unique morphology and ultrafine HA particles can be produced, and moreover, distributed homogeneously within the organic template. What's more, compared with other in situ precipitation methods, it is worth noting that this method had another important merit that the products had no other impure inorganic component except HA in composition.

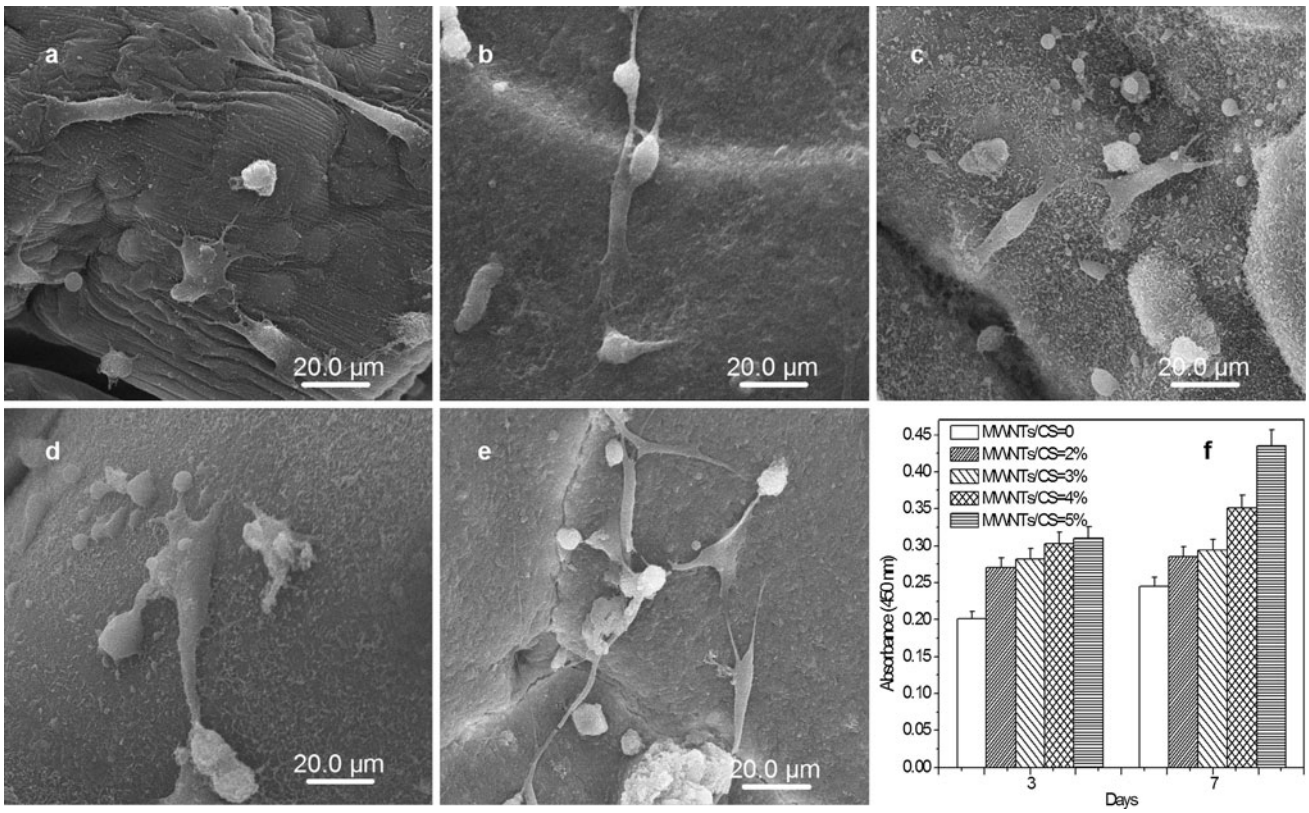

Fig. 5 SEM micrographs of MC3T3-E1 cell morphology on CS-MWNTs/HA composites with different MWNTs/CS weight ratios after incubation for 2 days: **a** blank, **b** MWNTs/CS = 2 %, **c** MWNTs/CS = 3 %, **d** MWNTs/CS = 4 %, **e** MWNTs/CS = 5 %, and **f** CCK-8 assay of the proliferation of MC3T3-E1 cells cultured on CS-MWNTs/HA composites with different MWNTs/CS weight ratios and blank control (n = 4)

In this study, we first dispersed MWNTs in chitosan via ultrasonic method. Due to nanotube–nanotube or van der Waals interactions, MWNTs can hardly be dispersed in any solvents and tend to aggregate. An easy solution for dispersing MWNTs is ultrasonic method. Salam et al. [47] employed ultrasonic method to obtain a homogenous multi-walled carbon nanotubes-modified-chitosan nanocomposite. The results showed that the MWNTs were well dispersed within chitosan matrix. Tang et al. [48] also used ultrasonication to prepare chitosan/MWNTs porous membranes. The purified MWNTs are rich in a large number of carboxyl groups which make it become the electron acceptor and be positively charged. Meanwhile, CS possesses some amino groups and is negatively charged. Thus, electrostatic attraction occurred between MWNTs and CS will be useful for MWNTs to disperse well in the CS. In Fig 2, we can see that after MWNTs sonication in the CS solution, it can be well dispersed in the CS solution for nine days.

After MWNTs sonication in the CS solution, in situ precipitation approach was employed to deposit HA in the hydrogel of CS-MWNTs. And as shown in Fig. 3c, the interface between the inorganic and organic phases was indistinguishable, because the inorganic crystals have a high affinity with the CS-MWNTs matrix. No delamination was observed between the inorganic phase and the organic phase. Here, in order to increase the mechanical strength of CS/HA composites, we introduced MWNTs into the CS/HA system. As far as we know, MWNTs own small dimensions, high aspect ratio (length to diameter), and high strength and stiffness. From the results of mechanical tests (Fig. 4), we can see that the elastic modulus and compressive strength increased evidently with the increase of MWNTs/CS weight ratios. Compared with the CS/HA composites, the CS-MWNTs/HA composites obviously exhibited higher stress at same strain. Nevertheless, there are few reports on the preparation of CS-MWNTs/HA composites. Venkatesan et al. [49] utilized mechanical mixing method to prepare chitosan grafted with functionalized multiwalled carbon nanotube in addition to HA (derived from Thunnus Obesus bone) scaffolds. Ezhova et al. [50] fabricated calcium hydroxylapatite–chitosan–multiwall carbon nanotubes nanocomposites through co-precipitation method. In these methods, inorganic particles could not be distributed within the organic matrices at nanolevel, so the mechanical properties of composite materials were weakened correspondingly.

Figure 5 shows the growth morphology of preosteoblast MC3T3-E1 cells either on CS-HA or CS-MWNTs/HA composites. As to the case of CS-HA specimen (Fig. 5a), the cells responded similarly to the CS-MWNTs/HA specimen (Fig. 5b–e), with good adherence on the underlying surface and active spreading with a number of filopodia protrusions. This result exactly corresponds with the findings of Lee et al. [51]. These experimental phenomena demonstrate that preosteoblast MC3T3-E1 cells attachment and adhesion on the surface of the CS-MWNTs/HA composites is good and the CS-MWNTs/HA composites possess non-cytotoxicity. Moreover, the cell proliferation of MC3T3-E1 on the CS-MWNTs/HA composites was observed to be higher than the CS-HA composites. Venkatesan et al. [49] also got the analogous outcome. Therefore, the favorable cell growth morphology and proliferation observed on the composites as well as mechanical and dispersive characteristics mentioned above suggest the possible use of the CS-MWNTs/HA composites for bone tissue engineering.

5 Conclusions

In summary, we have successfully fabricated chitosan–multiwalled carbon nanotubes/hydroxyapatite nanocomposites exhibiting excellent mechanical properties, good bioactivity and biocompatibility, which have met some required properties of extracellular matrix of bone. In addition, uniform distribution of HA particles and MWNTs in the polymer matrix was observed, which attribute to in situ precipitation. Based on above research, we make a conclusion that the CS-MWNTs/HA nanocomposites are promising biomaterials for bone tissue engineering.

Acknowledgments This research was supported by the National Natural Science Foundation of China (Nos. 31071265 and 30900297) and the Research Fund for the Doctoral Program of Higher Education (No. 20090141120055).

References

1. Murugan R, Ramakrishna S. Bioresorbable composite bone paste using polysaccharide based nano hydroxyapatite. Biomaterials. 2004;25:3829–35.
2. Shor L, Güçeri S, Wen XJ, Gandhi M, Sun W. Fabrication of three-dimensional polycaprolactone/hydroxyapatite. Biomaterials. 2007;28:5291–7.
3. Raucci MG, Guarino V, Ambrosio L. Hybrid composite scaffolds prepared by sol–gel method for bone regeneration. Compos Sci Technol. 2010;70:1861–8.
4. Peng F, Yu XH, Wei M. In vitro cell performance on hydroxyapatite particles/poly(L-lactic acid) nanofibrous scaffolds with an excellent particle along nanofiber orientation. Acta Biomater. 2011;7:2585–92.
5. Cheng L, Li Y, Zuo Y, Li J, Wang H. Nano-hydroxyapatite/polyamide 6 scaffold as potential tissue engineered bone substitutes. Mater Res Innov. 2008;12:192–9.
6. da Silva EE, Della Colleta HHM, Ferlauto AS, Moreira RL, Resende RR, Oliveira S, Kitten GT, Lacerda RG, Ladeira LO. Nanostructured 3-D collagen/nanotube biocomposites for future bone regeneration scaffolds. Nano Res. 2009;2:462–73.
7. Bhumiratana S, Grayson WL, Castaneda A, Rockwood DN, Gil ES, Kaplan DL, Vunjak-Novakovic G. Nucleation and growth of mineralized bone matrix on silk-hydroxyapatite composite scaffolds. Biomaterials. 2011;32:2812–20.
8. Ravi Kumar MNV, Muzzarelli RAA, Muzzarelli C, Sashiwa H, Domb AJ. Chitosan chemistry and pharmaceutical perspectives. Chem Rev. 2004;104:6017–84.
9. Zhang L, Li YB, Yang AP, Peng XL, Wang XJ, Zhang X. Preparation and in vitro investigation of chitosan/nano-hydroxyapatite composite used as bone substitute materials. J Mater Sci Mater Med. 2005;16:213–9.
10. Zhang Y, Ni M, Zhang MQ, Ratner B. Calcium phosphate–chitosan composite scaffolds for bone tissue engineering. Tissue Eng. 2003;9:337–45.
11. Tsai WB, Chena YR, Liu HL, Lai JY. Fabrication of UV-cross-linked chitosan scaffolds with conjugation of RGD peptides for bone tissue engineering. Carbohydr Polym. 2011;85:129–37.
12. Hu QL, Li BQ, Wang M, Shen JC. Preparation and characterization of biodegradable chitosan/hydroxyapatite nanocomposite rods via in situ hybridization: a potential material as internal fixation of bone fracture. Biomaterials. 2004;25:779–85.
13. Cooper A, Bhattarai N, Zhang MQ. Fabrication and cellular compatibility of aligned chitosan–PCL fibers for nerve tissue regeneration. Carbohydr Polym. 2011;85:149–56.
14. Xu HX, Yan YH, Li SP. PDLLA/chondroitin sulfate/chitosan/NGF conduits for peripheral nerve regeneration. Biomaterials. 2011;32:4506–16.
15. Zheng L, Cui HF. Use of chitosan conduit combined with bone marrow mesenchymal stem cells for promoting peripheral nerve regeneration. J Mater Sci Mater Med. 2010;21:1713–20.
16. Chen HL, Fan XQ, Xia J, Chen P, Zhou XJ, Huang J, Yu JH, Gu P. Electrospun chitosan-graft-poly (ε-caprolactone)/poly (ε-caprolactone) nanofibrous scaffolds for retinal tissue engineering. Int J Nanomed. 2011;6:453–61.
17. Wang JJ, Zeng ZW, Xiao RZ, Xie T, Zhou GL, Zhan XR, Wang SL. Recent advances of chitosan nanoparticles as drug carriers. Int J Nanomed. 2011;6:765–74.
18. Zhang L, Ao Q, Wang AJ, Lu GY, Kong LJ, Gong YD, Zhao NM, Zhang XF. A sandwich tubular scaffold derived from chitosan for blood vessel tissue engineering. J Biomed Mater Res A. 2006;77:277–84.
19. White AA, Best SM. Hydroxyapatite–Carbon nanotube composites for biomedical applications: a review. Int J Appl Ceram Technol. 2007;4(1):1–13.
20. Rapacz-Kmita A, Ślósarczyk A, Paszkiewicz Z. Mechanical properties of HAp–ZrO_2 composites. J Eur Ceram Soc. 2006;26:1481–8.
21. Huang M, Feng JQ, Wang JX, Zhang XD. Synthesis and characterization of nano-HA/PA66 composites. J Mater Sci Mater Med. 2003;14:655–60.
22. Cai ZX, Mo XM, Zhang KH, Fan LP, Yin AL, He CL, Wang HS. Fabrication of chitosan/silk fibroin composite nanofibers for wound-dressing applications. Int J Mol Sci. 2010;11:3529–39.
23. Cai X, Tong H, Shen XY, Chen WX, Yan J, Hu JM. Preparation and characterization of homogeneous chitosan–polylactic acid/hydroxyapatite nanocomposite for bone tissue engineering and evaluation of its mechanical properties. Acta Biomater. 2009;5:2693–703.

24. Hahn BD, Lee JM, Park DS, Choi JJ, Ryu J, Yoon WH, Lee BK, Shin DS, Kim HE. Mechanical and in vitro biological performances of hydroxyapatite–carbon nanotube composite coatings deposited on Ti by aerosol deposition. Acta Biomater. 2009;5: 3205–14.
25. Singh MK, Shokuhfar T, Gracio JJD, de Sousa ACM, Fereira JMD, Garmestani H, Ahzi S. Hydroxyapatite modified with carbon-nanotube-reinforced poly(methyl methacrylate): a nanocomposite material for biomedical applications. Adv Funct Mater. 2008;18:694–700.
26. Ding YJ, Liu J, Jin XY, Lu HX, Shen GL, Yu RQ. Poly-L-lysine/hydroxyapatite/carbon nanotube hybrid nanocomposite applied for piezoelectric immunoassay of carbohydrate antigen 19–9. Analyst. 2008;133:184–90.
27. Zhao HY, Xu XX, Zhang JX, Zheng W, Zheng YF. Carbon nanotube–hydroxyapatite–hemoglobin nanocomposites with high bioelectrocatalytic activity. Bioelectrochemistry. 2010;78:124–9.
28. Wahab R, Ansari SG, Kim YS, Mohanty TR, Hwang IH, Shin HS. Immobilization of DNA on nano-hydroxyapatite and their interaction with carbon nanotubes. Synth Met. 2009;159:238–45.
29. Bhattarai SR, Aryal S, Remant Bahadur KC, Bhattarai N, Hwang PH, Yi HK, Kim HY. Carbon nanotube-hydroxyapatite nanocomposite for DNA complexation. Mater Sci Eng C. 2008;28:64–9.
30. Shen XY, Tong H, Zhu ZH, Wan P, Hu JM. A novel approach of homogenous inorganic/organic composites through in situ precipitation in poly-acrylic acid gel. Mater Lett. 2007;61:629–34.
31. Shen XY, Tong H, Jiang T, Zhu ZH, Wan P, Hu JM. Homogeneous chitosan/carbonate apatite/citric acid nanocomposites prepared through a novel in situ precipitation method. Compos Sci Technol. 2007;67:2238–45.
32. Yamaguchi I, Tokuchi K, Fukuzaki H, Koyama Y, Takakuda K, Monma H, Tanaka J. Preparation and microstructure analysis of chitosan/hydroxyapatite nanocomposites. J Biomed Mater Res A. 2001;55:20–7.
33. Elliot JC. Structure and chemistry of the apatites and other calcium orthophosphates. In: Elliot JC, editor. Studies in inorganic chemistry. Amsterdam: Elsevier Science; 1994. p. 111.
34. Gosline JM, Guerette PA, Ortlepp CS, Savage KN. The mechanical design of spider silks: from fibroin sequence to mechanical function. J Exp Biol. 1999;202:3295–303.
35. Metzler V, Bienert H, Lehmann T, Mottaghy K, Spitzer K. A novel method for quantifying shape deformation applied to biocompatibility testing. ASAIO J. 1999;45:264–71.
36. Burchardt H. The biology of bone graft repair. Clin Orthop Relat Res. 1983;174:28–42.
37. Urist MR. Bone: transplants, implants, derivatives, and substitutes—a survey of research of the past decade. Instr Course Lect. 1960;17:184–95.
38. Hou CH, Yang RS, Hou SM. Hospital-based allogenic bone bank-10-year experience. J Hosp Infect. 2005;59:41–5.
39. Nishida J, Shimarnura T. Methods of reconstruction for bone defect after tumor excision: a review of alternatives. Med Sci Monit. 2008;14:RA107–13.
40. Pu XM, Sun ZZ, Hou ZQ, Yang Y, Yao QQ, Zhang QQ. Fabrication of chitosan/hydroxylapatite composite rods with a layer-by-layer structure for fracture fixation. J Biomed Mater Res Part B. 2012;100B:1179–89.
41. Fan JJ, Bi L, Wu T, Cao LG, Wang DX, Nan KH, Chen JD, Jin D, Jiang S, Pei GX. A combined chitosan/nano-size hydroxyapatite system for the controlled release of icariin. J Mater Sci Mater Med. 2012;23:399–407.
42. Ito M. In vitro properties of a chitosan-bonded hydroxyapatite bone filling past. Biomaterials. 1991;12:41–5.
43. Kawakami T, Antoh M, Hasegawa H, Yamagichi T, Ito M, Eda S. Experimental study on osteoconductive properties of chitosan-bonded hydroxyapatite self-hardening paste. Biomaterials. 1992;13:759–63.
44. Zhang XB, Zhu LX, Lv H, Cao YL, Liu Y, Xu Y, Ye WM, Wang J. Repair of rabbit femoral condyle bone defects with injectable nanohydroxyapatite/chitosan composites. J Mater Sci Mater Med. 2012;23:1941–9.
45. Li B, Huang LN, Wang XB, Ma JH, Xie F, Xia L. Effect of micropores and citric acid on the bioactivity of phosphorylated chitosan/chitosan/hydroxyapatite composites. Ceram Int. 2013;39:3423–7.
46. Tachaboonyakiat W, Serizawa T, Akashi M. Hydroxyapatite formation on/in biodegradable chitosan hydrogels by an alternate soaking process. Polym J. 2001;33:177–81.
47. Salam MA, Makki MSI, Abdelaal MYA. Preparation and characterization of multi-walled carbon nanotubes/chitosan nanocomposite and its application for the removal of heavy metals from aqueous solution. J Alloy Compd. 2011;5:2582–7.
48. Tang CY, Zhang Q, Wang K, Fu Q, Zhang CL. Water transport behavior of chitosan porous membranes containing multi-walled carbon nanotubes (MWNTs). J Membr Sci. 2009;337:240–7.
49. Venkatesan J, Qian ZJ, Ryu BM, Kumar NA, Kim SK. Preparation and characterization of carbon nanotube-grafted-chitosan-natural hydroxyapatite composite for bone tissue engineering. Carbohydr Polym. 2010;2:569–77.
50. Ezhova ZA, Zakharov NA, Koval EM, Kalinnikov VT. Synthesis and physicochemical characterization of nanocomposites of calcium hydroxylapatite-chitosan-multiwall carbon nanotubes. Russ J Inorg Chem. 2013;3:269–73.
51. Lee HH, Shin US, Won JE, Kim HW. Preparation of hydroxyapatite-carbon nanotube composite nanopowders. Mater Lett. 2011;65:208–11.